

## MIT Open Access Articles

*Effects of Hydrophobic Surface Patterning on Boiling Heat Transfer and Critical Heat Flux of Water at Atmospheric Pressure*

The MIT Faculty has made this article openly available. **Please share** how this access benefits you. Your story matters.

**Citation:** Coyle, Carolyn, Harry O'Hanley, Bren Phillips, Jacopo Buongiorno, and Thomas McKrell. "Effects of Hydrophobic Surface Patterning on Boiling Heat Transfer and Critical Heat Flux of Water at Atmospheric Pressure." Volume 2: Reliability, Availability and Maintainability (RAM); Plant Systems, Structures, Components and Materials Issues; Simple and Combined Cycles; Advanced Energy Systems and Renewables (Wind, Solar and Geothermal); Energy Water Nexus; Thermal Hydraulics and CFD; Nuclear Plant Design, Licensing and Construction; Performance Testing and Performance Test Codes (July 29, 2013), Boston, Massachusetts, USA, ACME. © 2013 by ASME

**As Published:** <http://dx.doi.org/10.1115/POWER2013-98146>

**Publisher:** ASME International

**Persistent URL:** <http://hdl.handle.net/1721.1/117084>

**Version:** Final published version: final published article, as it appeared in a journal, conference proceedings, or other formally published context

**Terms of Use:** Article is made available in accordance with the publisher's policy and may be subject to US copyright law. Please refer to the publisher's site for terms of use.



**POWER2013-98146**

**EFFECTS OF HYDROPHOBIC SURFACE PATTERNING ON BOILING HEAT TRANSFER AND CRITICAL HEAT FLUX OF WATER AT ATMOSPHERIC PRESSURE**

**Carolyn Coyle\***

Dept. of Mechanical Engineering  
Massachusetts Institute of Technology  
Boston, Massachusetts, 02139

**Harry O'Hanley**

Dept. of Nuclear Engineering  
Massachusetts Institute of Technology  
Boston, Massachusetts, 02139

**Bren Phillips**

Dept. of Nuclear Engineering  
Massachusetts Institute of Technology  
Boston, Massachusetts, 02139

**Jacopo Buongiorno**

Dept. of Nuclear Engineering  
Massachusetts Institute of Technology  
Boston, Massachusetts, 02139

**Thomas McKrell**

Dept. of Nuclear Engineering  
Massachusetts Institute of Technology  
Boston, Massachusetts, 02139

**ABSTRACT**

*The effects of hydrophilic/hydrophobic surface patterning on critical heat flux (CHF) and heat transfer coefficient (HTC) were studied using custom-engineered testing surfaces. Patterning was created over a sapphire substrate and tested in a pool boiling facility in MITs Reactor Hydraulics Laboratory. The hydrophilic and hydrophobic matrices were created using layer by layer deposition of 50 nm thick SiO<sub>2</sub> nanoparticles and monolayer thickness fluorosilane, respectively. Ultraviolet ozone patterning was then used with chrome-printed masks to create the desired geometric features. Hexagon, ring, star, and mixed patterns were tested to determine their abilities to affect CHF and HTC through prevention of bubble pinning at high heat fluxes. During testing, an infrared camera was used to measure the surface temperature distribution as well as locate nucleation sites for data analysis. It was found that CHF values were enhanced over the bare sapphire values by approximately 90% for hexagons, 60% for stars, 65% for rings, and 50% for mixed patterns. Contrary to expectations, patterning did not seem to affect the HTC values significantly. Although patterning did improve CHF performance over bare heaters, both CHF and HTC were found to be sta-*

*tistically similar to those for unpatterned, uniformly hydrophilic surfaces.*

**INTRODUCTION**

Boiling is a common mechanism of heat transfer in many power generation systems. The efficiency of the heat transfer of a system is affected by the surfaces ability to move heat from a source into a working fluid. As a result, it is beneficial to design efficient heat transfer surfaces in the nucleate boiling regime where many of these systems operate. Two common figures of merit for nucleate boiling heat transfer are the critical heat flux (CHF) and the heat transfer coefficient (HTC). The HTC captures the ability of the fluid to transfer heat efficiently (i.e. with a small temperature difference), while the Critical heat flux marks the transition from the nucleate boiling regime to the film boiling regime causing a large reduction in the HTC [1], and thus can be considered the upper limit of efficient boiling heat transfer

Work has been conducted on optimizing the boiling heat transfer properties of surfaces. By altering properties such as surface roughness, wettability, and porosity, substantial enhancements in CHF and/or HTC have been recorded [2–4]. The suc-

---

\*Corresponding author: cpcoyle@mit.edu

cess of these methods have been attributed to an increased density of nucleation sites as well as increased rewetting of the heater surfaces, causing a greater HTC and delay in CHF [2]. In the past decade the effects of nanofluids on boiling have been investigated. While originally inserted as part of the working fluid, tests that deposit nanoparticles directly on the heater surface have similarly resulted in enhancements in CHF and HTC [2–6]. Nanoparticle deposits have been found to increase wettability and capillarity, allowing for operation in the nucleate boiling regime at higher heat fluxes [7].

Most recently, work has begun on creating hydrophilic and hydrophobic networks to test for enhanced properties. Studies of hydrophilic spots on hydrophobic surfaces (hydrophilic network) and hydrophobic spots on hydrophilic surfaces (hydrophobic network) have been examined with circular and hexagonal spot patterns [2–4]. In one study, it was found that using hexagonal spots of diameters between 40% and 60% of a varying pitch between 50 and 200- $\mu\text{m}$ , CHF and HTC were increased by 65% and 100% respectively over purely hydrophilic surfaces [4].

These approaches of creating surface features using nanofluids or hydrophilic and hydrophobic patterning have been successful in increasing the efficiency of boiling heat transfer. However, while the spot diameter and pitch have been used to explore enhancements in CHF and HTC, the shape of the spots has not been exhaustively studied.

In this work, hexagonal, star, ring, and mixed shape hydrophobic networks have been studied in a pool boiling facility, to determine their effects on the enhancements of CHF and HTC. These shapes were chosen to test their abilities to increase bubble nucleation and prevent pinning of the bubble base, thus encouraging bubble departure from the heater surface through sharp corners and secondary regions.

## BACKGROUND

Pool boiling occurs when the heater surface is submerged in a stagnant body of fluid. In pool boiling there exist various heat transfer regimes. Initially at low heat fluxes, heat transfer is dominated by natural convection, seen in Figure 1 in the region from Point A to B [2]. As the heat flux increases, the fluid transitions into the nucleate boiling regime, seen from Point B to C. The nucleate boiling regime has a steep slope on the boiling curve, suggesting a high value of the heat transfer coefficient, defined by Newton's law of cooling:

$$q'' = h[T_{wall} - T_{bulk}] \quad (1)$$

where  $q$  is the heat flux,  $h$  is the heat transfer coefficient (HTC),  $T_{wall}$  is the surface temperature, and  $T_{bulk}$  is the working fluid temperature or, in the case of boiling,  $T_{sat}$ . In the case of pool boiling testing,  $h$  will often be temperature dependent [2]. However, at

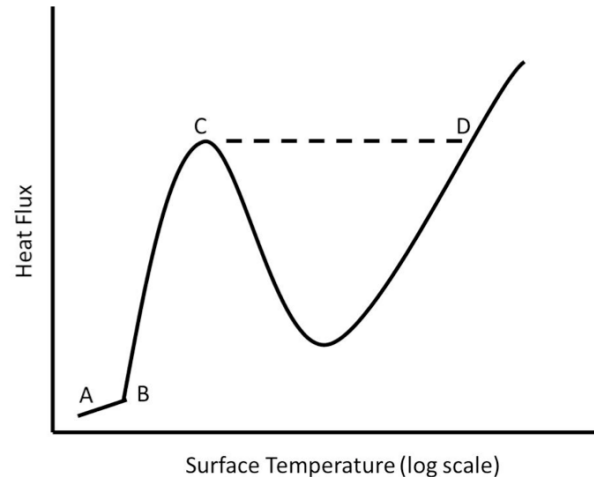


FIGURE 1. STANDARD POOL BOILING CURVE [2].

Point C, critical heat flux (CHF) is achieved and, if the heat flux continues to rise, the fluid moves to Point D in the film boiling regime. In this regime, a thin vapor layer forms on the heater surface, resulting in greatly increased surface temperatures, often causing failure of the heater. As a result, it is crucial to know the value of CHF for the given heater in use.

Several models for predicting CHF have been postulated, each with their own benefits. Zuber [8] predicts CHF using a purely hydrodynamic instability model, as seen in Eqn. (2). In the following equation,  $q''_{CHF}$  is defined as the critical heat flux,  $K$  is a dimensionless constant dependent on surface geometry, and  $h_{fg}$  is the latent heat of vaporization.

$$q''_{CHF} = K\rho_g h_{fg} \left[ \frac{g\sigma(\rho_f - \rho_g)}{\rho_g^2} \right]^{\frac{1}{4}} \quad (2)$$

This model, however, fails to account for surface features, which have been determined to greatly affect CHF.

Other correlations have also been created that account for individual surface features such as wettability and porosity, but none have yet been created to predict the effects of spot patterning [9, 10]. While there is not yet a model able to capture all the physical mechanisms at work in these boiling phenomena, the correlations listed above do provide qualitative trends for the various effects of the surface parameters.

## EXPERIMENTAL METHODS

### Manufacturing Surface Patterns

Indium tin oxide-sapphire (ITO) heaters were used as the base for the heater surfaces, shown in Figure 2. These heaters

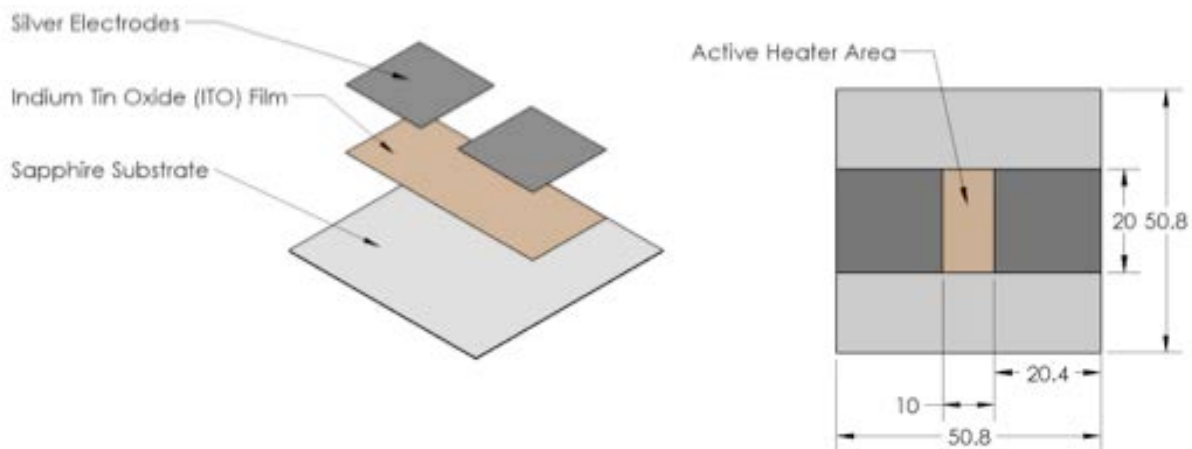


**FIGURE 2.** ITO-SAPPHIRE HEATER SCHEMATIC WITH MATERIALS AND DIMENSIONS IN MM [2].

are made of  $50.8 \times 50.8\text{-mm}^2$ , square piece of sapphire 0.25-mm thick. A 2-cm wide and 700-nm thick layer of ITO is centered along the length of the sapphire and two silver pads 25- $\mu\text{m}$  thick are located on the ends of the ITO. The ITO acts as a resistive heating element while the silver pads provide attachment points for electrical leads. The following methods describe the process by which the hydrophobic networks were created.

**Layer by Layer Deposition** Layer by layer deposition (LBL) is the process of laying a single layer of nanoparticles on a substrate [11]. A durable LBL coating able to withstand boiling temperatures was created by dipping heater surfaces first in a positively charged poly(allylamine) (PAH) solution followed by a negatively charged 50-nm silica ( $\text{SiO}_2$ ) nanoparticle solution. This process was repeated fifty times to create a hydrophilic bilayer of 1.4 microns with a contact angle of less than 5 degrees on the heater surface [3].

**Chemical Vapor Deposition of Fluorosilane** To create a hydrophobic layer, chemical vapor deposition (CVD) was used. A small volume of liquid fluorosilane was placed in a closed container with the heater surfaces and baked in an oven at  $140^\circ\text{C}$  for thirty minutes. This procedure vaporizes the fluorosilane and creates an even, hydrophobic layer on the heater surface above the hydrophilic bilayer of static contact angle greater than 135 degrees.

**Ultraviolet Ozone Patterning** Ultraviolet Ozone (UVO) patterning was used to create the hydrophilic and hydrophobic regions. A quartz mask was ordered with a chromium

pattern of the desired hydrophobic regions. The mask was placed on the ITO heater and exposed for two hours. During this time, ultraviolet light passes through the quartz, breaking down the fluorosilane and exposing the hydrophilic layer while the fluorosilane in contact with the chromium is protected. These four masks like the one in Figure 3 were used to create the hexagon, star, ring, and mixed patterned heater surfaces, each with a respective 260- $\mu\text{m}$  spot diameter and 1.5-mm pitch.

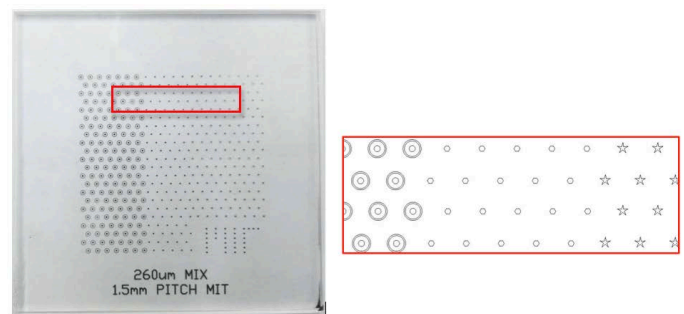


**FIGURE 3.** MIXED PATTERN QUARTZ MASK WITH 260- $\mu\text{M}$  DIAMETER AND 1.5-MM PITCH PATTERNED CHROMIUM WITH EXPANDED SHAPE VIEW. LEFT TO RIGHT: RINGS, HEXAGONS, STARS. OTHER MASKS ARE SAME LAYOUT WITH A SINGLE SHAPE.

### Apparatus and Procedure

Tests were conducted in the pool boiling facility (PBF) shown in Figures 4 and 5. Patterned ITO heater surfaces with

leads were attached to borosilicate tubes, inserted above a square hole in the center of the inner bath, and sealed using a silicone gel gasket.



**FIGURE 4.** PBF IN MIT REACTOR HYDRAULICS LABORATORY.

This inner bath as well as an outer bath were filled with tap water heated to 100°C to create an adiabatic environment while the working fluid was deionized water, which filled the borosilicate tube above the active heater area. The electrical leads from the heater were attached to an Electronic Measurements Inc. TCR Power Supply. The heat flux was calculated using an Agilent Technologies 34980A data acquisition system also connected to the circuit through the power supply. A gold mirror at a 45° angle was then placed under the heater to allow a FLIR Sc6000 IR camera to record the full 2D temperature profile of the bottom of the ITO heater, as sapphire and ITO are transparent and opaque to infrared light, respectively.

The ITO was imaged using the IR camera at increasing heat fluxes until the point of failure (CHF) where the sapphire substrate breaks. Figure 6 below shows two IR image taken, one of a bare heater without patterning and one of a star pattern where the effect of the spot patterning on bubble nucleation is visible.

### Data Processing

To create the boiling curves for the tests, IR camera videos are exported into Flexible Image Transport System (FITS) files. These files are then imported into Matlab where they are analyzed and average ITO surface temperatures are calculated using experimentally gathered calibration information. These temperatures are then used to calculate the average heater surface temperature by accounting for conduction through the sapphire.

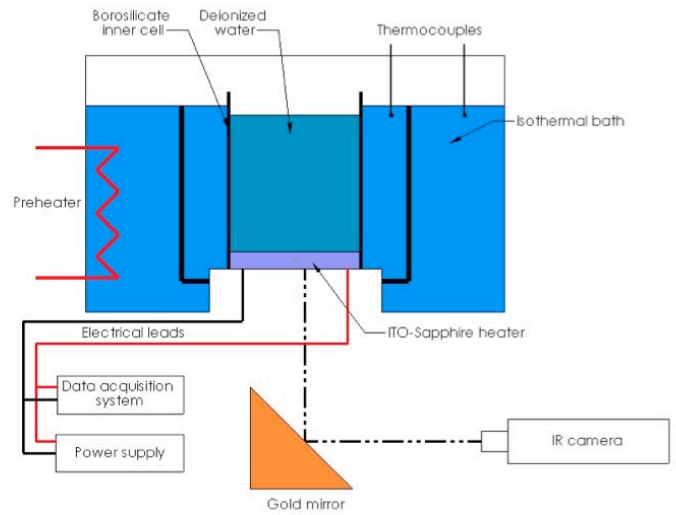


**FIGURE 5.** PBF EXPERIMENTAL SETUP [2].

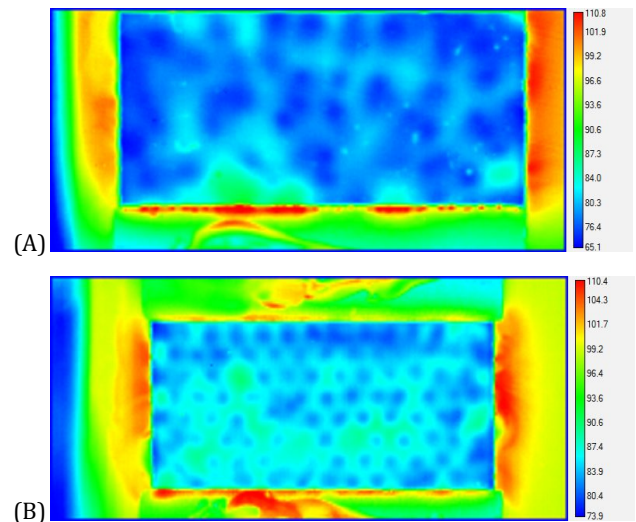


**FIGURE 6.** SURFACE TEMPERATURE IMAGES OF (A) BARE AND (B) STARS-3 HEATERS AT 800 AND 1500 KW/M<sup>2</sup> HEAT FLUXES, RESPECTIVELY (NEAR POINTS OF FAILURE).

### RESULTS

Table 1 shows the CHF results of individual, ITO heater surface tests. These CHF values are found from the heat flux at which the ITO undergoes material failure.

Figure 7(A) shows the boiling curves for each of the heaters, including bare and pure hydrophilic heaters for comparison. These were obtained from the IR camera video taken at each of the indicated heat fluxes. In the figure, the natural convection

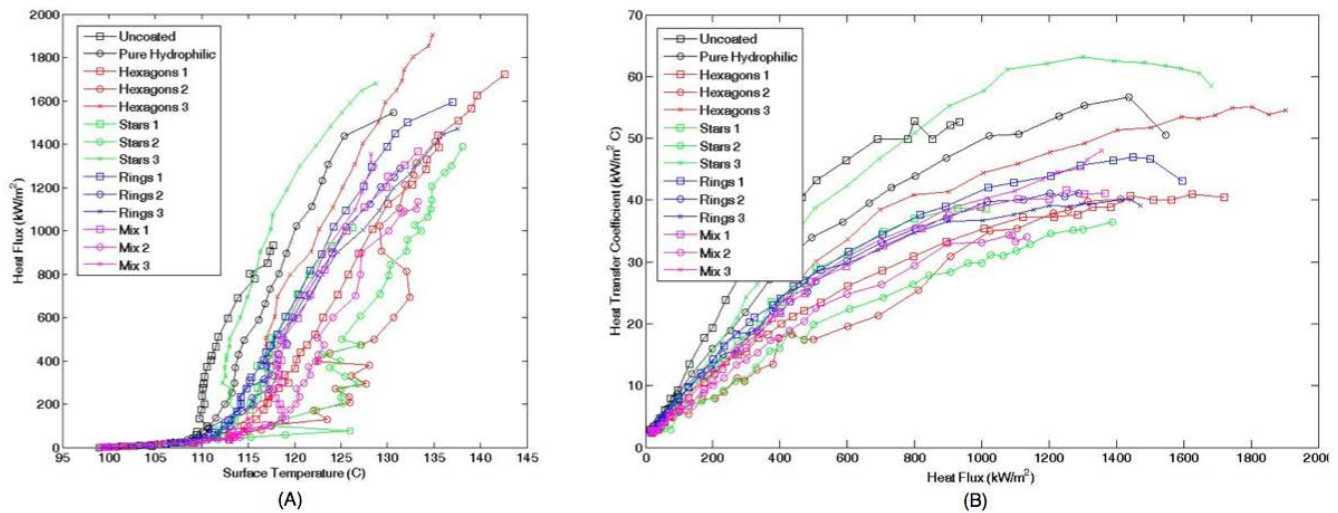


**FIGURE 7.** (A) INDIVIDUAL BOILING CURVES FOR BARE, PURE HYDROPHILIC, HEXAGON, STAR, RING, AND MIXED PATTERNED HEATERS. (B) INDIVIDUAL HTC CURVES FOR BARE, PURE HYDROPHILIC, HEXAGON, STAR, RING, AND MIXED PATTERNED HEATERS. UNCERTAINTIES IN HEAT FLUX RESULT FROM ELECTRONIC MEASUREMENTS INC. TCR POWER SUPPLY WITH REGULATION AND STABILITY UNCERTAINTIES OF 0.1% AND 0.05%.

**TABLE 1.** INDIVIDUAL AND AVERAGE CHF VALUES FOR ITO PATTERNED HEATERS.

Pattern	CHF(kW/m <sup>2</sup> )	Avg. CHF(kW/m <sup>2</sup> )	St. Dev
Hexagons-1	1760		
Hexagons-2	1412	1691	14.9%
Hexagons-3	1903		
Stars-1	1099		
Stars-2	1384	1387	20.9%
Stars-3	1680		
Rings-1	1596		
Rings-2	1289	1452	10.6%
Rings-3	1470		
Mixed-1	1458		
Mixed-2	1161	1333	11.5%
Mixed-3	1380		

regime (Figure 1, Point A to B) is visible, followed by the nucleate boiling regime (Figure 1, Point B to C). Figure 7(B) shows the HTC curves for each of the heaters, created using a Matlab

data analysis file and Eq. 1.

## DISCUSSION

The above results suggest that shape spot patterning does not greatly enhance CHF. Using the same experimental setup and ITO heaters, O’Hanley [2] measured average CHF values of 873 kW/m<sup>2</sup>, 1009 kW/m<sup>2</sup>, and 1617 kW/m<sup>2</sup> for uncoated, non-porous hydrophilic, and porous hydrophilic heaters. He also conducted experiments using circular hydrophobic network spot patterning and, for 260- $\mu$ m diameter and 1.5-mm pitch spots, measured an average CHF value of 1612 kW/m<sup>2</sup> [2]. These experiments have supported those results. Shape spot pattern heaters have a 50% to 90% enhancement in CHF over uncoated heaters, but little to no enhancement in CHF over unpatterned hydrophilic heaters. The variations in CHF among the different patterns themselves, however, do provide some insight into bubble departure from the heater surface. While it was hypothesized that sharp corners or rings could prevent bubble base pinning to the surface and thus promote bubble departure and postpone CHF, the results do not support that hypothesis. In fact, the CHF value decreases as the shapes increasingly deviate from a pure circle.

Patterned HTC values similarly recorded little to no enhancement over the unpatterned hydrophilic surfaces, but also lacked enhancements over bare heaters. Bare, unpatterned, and patterned heaters saw peaks of around 60 kW/m<sup>2</sup>C with averages between 30-40 kW/m<sup>2</sup>C. Among the patterned heaters, HTC values were fairly close, though variations even among identical

heater patterns were observed, possibly as an inherently varying feature of porosity. To better understand the nature of these differences, an investigation of the dependence of bubble departure frequency and bubble departure diameter on pattern shape must be conducted.

At this time it can be stated that while hydrophobic spots do serve as preferential nucleation sites on the heater surface (as verified directly with the IR images, see Fig. 6(B)), they do not seem to allow for increased rewetting of the heater surface and are therefore not as efficient at removing heat as the unpatterned hydrophilic surface. While studies have shown enhancement in CHF and HTC over purely hydrophilic surfaces [4], porosity is perhaps the greater contributor to efficiency in these tests, as shown in the separate-effect study of O'Hanley [2]. Further investigation into the effects of spot patterning on uncoated or non-porous heaters may show a greater enhancement in boiling efficiency.

## CONCLUSIONS

A study into the effects of hydrophobic spot patterning of hexagons, rings, and stars on hydrophilic surface was conducted to determine their effects on pool boiling efficiency, as captured by CHF and HTC. Special-design surface heaters were manufactured with the desired features and tested with water in a pool boiling facility at atmospheric pressure. 2D surface temperatures images were recorded using an IR camera.

It was found that spot patterning of hydrophobic regions of all shapes did not enhance CHF and HTC over unpatterned hydrophilic surfaces. However, CHF was higher for spots of near-circular shape, while HTC remained unaffected.

## REFERENCES

- [1] R.A. Knief. *Nuclear Engineering: Theory and Technology of Commercial Nuclear Power*. American Nuclear Society, 2nd edition, 2008.
- [2] Harry O'Hanley. Separate effects of surface roughness, wettability and porosity on boiling heat transfer and critical heat flux and optimization of boiling surfaces. Masters thesis, Department of Nuclear Science and Engineering, Massachusetts Institute of Technology, 2012.
- [3] Bren Phillips. Nano-engineering the boiling surface for optimal heat transfer rate and critical heat flux. Masters thesis, Department of Nuclear Science and Engineering, Massachusetts Institute of Technology, 2011.
- [4] Xu J. Qiu H. Attinger D Betz, A.R. Do surfaces with mixed hydrophilic and hydrophobic areas enhance pool boiling? *Applied Physics Letters*, 27:141909, 2010.
- [5] J. Buongiorno S.J. Kim, I.C. Bang and L.W. Hu. Effects of nanoparticle deposition on surface wettability influencing boiling heat transfer in nanofluids. *Applied Physics Letters*, 98:071908, 2010.
- [6] J.B. Kim H.D. Kim and M.H. Kim. Effect of nanoparticles on CHF enhancement in pool boiling of nano-fluids. *Int. J. Heat Mass Transfer*, 49:5070-5074, 2006.
- [7] H.D. Kim and M.W. Kim. Effect of nanoparticle deposition on capillary wicking that influences the critical heat flux in nanofluids. *Applied Physics Letters*, 91:014104, 2007.
- [8] Dweitt Theodore L. Bergman, Frank P. Incropera, David P and Adrienne S. Lavine. *Fundamentals of Heat and Mass Transfer 6th ed.* John Wiley and Sons, 2007.
- [9] Y.V. Polezhaev and S.A. Kovalev. Modeling heat transfer with boiling on porous structures. *Thermal Engineering*, 12:617620, 1990.
- [10] V. Mizo S. Kandlikar and M. Cartwright. Investigation of bubble departure mechanism in subcooled flow boiling of water using high speed photography. In John C. Chen, editor, *Convective Flow Boiling*. Taylor and Francis Group, 1996.
- [11] Michael F. Rubner, Daeyeon Lee, and Robert E. Cohen. All-nanoparticle thin-film coatings. *Nano Letters of American Chemical Society*, 6(10):23052312, 2006.